PHYSICAL REVIEW B VOLUME 53, NUMBER 12 15 MARCH 1996-II

Microscopic study of the pressure-induced structural phase transition of ZnTe

Gun-Do Lee and Jisoon Ihm
Department of Physics and Center for Theoretical Physics, Seoul National University, Seoul 151-742, Korea

(Received 23 October 1995)

We have performed *ab initio* pseudopotential calculations within the local-density approximation to investigate the structural phase transition of ZnTe under pressure. By calculating the total energy, atomic forces, and stress tensors, we theoretically determine the structural phase transition of ZnTe from the zinc-blende to the cinnabar to the orthorhombic structure under increasing pressure, which agrees well with experiment. We demonstrate that rotation of bonds toward lower-symmetry positions occurs at the critical pressure to relieve excessive strain.

Recently, Nelmes *et al.* reported that the cinnabar phase, which was supposed to be the structure of mercury compounds exclusively, also exists in CdTe (Refs. 1 and 2) and ZnTe (Ref. 3) under applied pressure, creating a lot of interest among both experimentalists and theorists in the structural stability of II-VI semiconductors under pressure. Since *ab initio* pseudopotential calculations were successfully performed in the past to study structural phase transitions of certain group IV and III-V semiconductors, we attempted to apply the same method to the structural phase transitions of ZnTe in the present study. Once we started the calculation, however, the following points became evident, indicating that the study of ZnTe is more than a simple extension of group IV or III-V semiconductors. First, in order to determine the atomic and electronic structure of ZnTe accurately, we found it essential to include the Zn 3d and Te 4d orbitals in the valence band, which enormously increases the number of plane waves in the basis set. Scattering properties of the core represented by the pseudopotential were required to agree with the all-electron calculations very precisely to produce meaningful results. Second, competing crystal structures under applied pressure were found to be complicated and to have large unit cells. It means that there are many structural parameters to vary and not only total energy but also atomic forces and stress tensors need to be calculated to determine the equilibrium configuration of the material. Truly, theoretical determination of the structural change at the pressure-induced phase transition of II-VI semiconductors, ZnTe in particular, is a challenging problem that can test the accuracy of the state-of-the-art computational method. We will show below that the accuracy of our method is better than 1 mRy per atom in energy difference between different crystal structures and our calculation agrees with experiment whenever measured data are available.

We have investigated those structures appearing in experiment (zinc blende, cinnabar, and $Cmcm$) as well as other possibly competing structures (wurtzite, NaCl, β-tin, CsCl, and NiAs), each structural parameter optimized through the calculation of Hellman-Feynman forces[4] and stress tensors.[5,6] Our calculations are performed in the framework of the density-functional theory within the local-density approximation (LDA) of Ceperley and Alder[7] as parametrized by Perdew and Zunger.[8] We generate relatively soft norm-conserving pseudopotentials using the scheme of Troullier and Martins.[9] We consider the Zn 3d and Te 4d orbitals as part of the valence states. These pseudopotentials are cast into the fully nonlocal separable form of Kleinman and Bylander[10] and the absence of the ghost states[11] is checked. The partial core correction[12] (PCC) is used for the Te pseudopotential (further core corrections for Zn are unnecessary). We have found that, as far as the PCC is already included, the generalized gradient correction[13] only impairs the results and should not be included simultaneously. The total energy of the system is calculated by means of the momentum-space formalism.[4] To minimize the total energy, we carry out the force and stress calculations for each volume of the β-tin, cinnabar, and $Cmcm$ phases. Increasing E_{cut} to 144 Ry gives the good convergence of total energy (<0.1 mRy/ZnTe) for each structure compared with the maximum E_{cut} of 196 Ry tested in the present work. The *relative* energy among different structures is found to be stable within 0.8 mRy/ZnTe as long as E_{cut} is above 80 Ry. This number (0.8 mRy) is further reduced when comparison is made between similar structures although the absolute magnitude of the total energy converges to only 10 mRy/ZnTe. Thus, we include the plane waves up to the cutoff energy of 81 Ry in the basis set. The typical number of plane waves is ~5000, ~10 000, ~4000, ~4000, ~9000, ~4000, ~11 000, or ~13 000 for the zinc-blende, wurtzite, CsCl, NaCl, NiAs, β-tin, cinnabar, or $Cmcm$ phase.

The calculated total-energy curves for the eight phases are illustrated in Fig. 1. The figure shows that the zinc-blende structure is the most stable one under ambient pressure. Since the pressure-induced phase transition of usual semiconductors, including ZnTe, is known to be insensitive to temperature (at least up to room temperature) experimentally, it is a common practice to neglect the entropy contribution ($-TS$) to the Gibbs free energy and minimize the enthalpy H ($=E+PV$) to predict the transition. The pressure-induced transition occurs along the common tangent line connecting the tangential points on the two total-energy curves. The negative of its slope is the critical pressure P_c. The transition from the zinc-blende to the cinnabar phase has the smallest P_c (8.06 GPa) among the plausible pressure-induced phases we study. The structure further transforms to the orthorhombic structure with the $Cmcm$ symmetry at 10.24 GPa. With increasing hydrostatic pressure, the structure of ZnTe follows the path 1→2→3→4→5→6 as shown

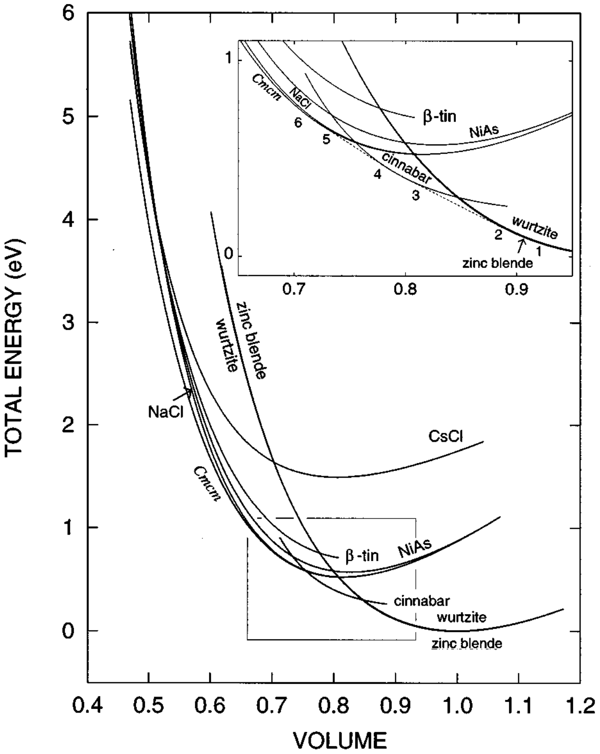

FIG. 1. Total-energy curves of the eight phases of ZnTe. The ordinate is the energy per ZnTe basis relative to the minimum total energy of the zinc-blende structure and the volume is normalized with repect to the equilibrium volume of the zinc-blende structure, 383.634a_B^3/ZnTe basis. Dashed lines are common tangents to two energy curves.

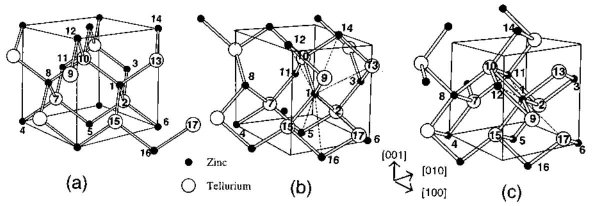

FIG. 2. The atomic positions in each ZnTe structure. We draw the positions with respect to a cube to help visualize the structure. Note that the cube is not a unit cell for ZnTe II or ZnTe III. (a) ZnTe I structure (side length of the cube = 5.868 Å); (b) ZnTe II structure (side length of the cube = 5.769 Å); (c) ZnTe III structure (side length of the cube = 5.718 Å). Dashed lines indicate near bonds. Characteristic features of the atomic movement at phase transition are described in the text.

in the inset of Fig. 1. The path 2→3 represents a mixture of the zinc-blende and cinnabar phases and the path 4→5 represents that of the cinnabar and *Cmcm* phases. The calculated critical volumes and critical pressures are given in Table I along with experimental values. The differences between theory and experiment are only 0.62% for V_c^{cinn1}, 0.77% for V_c^{cinn2}, and 1.10% for V_c^{Cmcm}. The critical pressures have a larger discrepancy (9.4% for zinc blende →cinnabar and 11.0% for cinnabar→*Cmcm*). This is a typical error of the calculation for a quantity involving derivatives. Also note that the calculated critical pressures are for the zero temperature while experiments were done at room temperature. The calculated P_c is quite sensitive to a small error in energy. If the total-energy curve of the cinnabar phase were to shift up by as little as 1 mRy, the P_c's would change to 8.46 GPa (4.8% increase) and to 9.58 GPa (6.4% decrease) for zinc-blende→cinnabar and cinnabar→*Cmcm* transitions, respectively. On the other hand, the volume changes would be as small as −0.43% for V_c^{ZB}, −0.33% for V_c^{cinn1}, +0.85% for V_c^{cinn2}, and +0.73% for V_c^{Cmcm}. If the upshift of the curve were ~2 mRy, the two P_c's would collapse and the cinnabar phase would disappear. The agreement in P_c between theory and experiment with ~10% error indicates that the accuracy in the energy difference between different crystal structures is better than 1 mRy/atom. We believe we have reduced all controllable errors (originated from the pseudopotential method and the incomplete convergence) to within this number as explained above. It means that the error bar inherent in the LDA, which is practically the only approximation left over, is also within the same number. Since this is an upper bound, the actual error in the LDA may even be much smaller than this amount; the LDA gives a much better description of the ground-state total energy of ordinary (non-strongly-correlated) materials than generally recognized. Now each phase is described in more detail.

TABLE I. Comparison of the calculated and measured (Ref. 3) critical volumes (V_c^{ZB}, V_c^{cinn1}, V_c^{cinn2}, and V_c^{Cmcm}), and the critical pressures (P_c). Volumes are normalized to the calculated zero-pressure volume of the zinc-blende structure.

	V_c^{ZB}	V_c^{cinn1}	P_c (GPa)	V_c^{cinn2}	V_c^{Cmcm}	P_c (GPa)
Calc.	0.889	0.799	8.06	0.783	0.723	10.24
Expt.		0.804	8.9	0.777	0.731	11.5

ZnTe I–zinc-blende phase. The zinc-blende structure in Fig. 2(a) occurs naturally as a mineral in most III-V and II-VI semiconductors. We have previously calculated the structural properties of zinc-blende ZnTe.[14] We have obtained $a_0 = 6.1026$ Å for the lattice constant for ZnTe, in excellent agreement with the experimental value of 6.1037 Å. Just before the zinc-blende phase is transformed to the cinnabar phase at 8.09 GPa, the lattice constant is 5.868 Å and the volume is reduced by 11.0% relative to the equilibrium volume.

ZnTe II–cinnabar phase. Cinnabar (HgS) has a hexagonal structure and this structure has long been thought to be a peculiarity of the mercury chalcogenides, until recenty. Now ZnTe II is identified as having the cinnabar structure built up of infinite Zn-Te-Zn-Te spiral chains [e.g., atoms 5-2-1-10-14 in Fig. 2(b)] running parallel to the *c* axis of the hexagonal unit cell. The cinnabar structure may be viewed as a distorted NaCl structure, too. According to the convention in the literature,[15] there are two *a* bonds (consisting of atoms 1-2 and atoms 1-9) between nearest neighbors on the spirals, two *b* bonds (1-10 and 1-15) in adjacent spirals, two *c* bonds (1-13 and 1-17) between different atoms in adjacent spirals, and four *d* bonds (1-5, 1-12, 1-14, and 1-16) between the same atoms in adjacent spirals. Because *a* and *b* bond

TABLE II. Calculated lattice parameters, c/a ratio, u and v atomic coordinates, and bond lengths for the cinnabar phase ZnTe at various pressures. Experimental results at 8.9 GPa, and 11.5 GPa from Ref. 16 are given for comparison. Volumes are normalized to the calculated zero-pressure volume of the zinc-blende structure.

	Calculation			Experiment	
Volume	0.799	0.791	0.786		
Pres. (GPa)	8.07	9.16	10.0	8.9	11.5
a (Å)	4.0904	4.0791	4.0663	4.105	4.085
c (Å)	9.4084	9.3579	9.3652	9.397	9.315
c/a	2.3001	2.2941	2.3031	2.2891	2.2803
u	0.519	0.519	0.519	0.540	
v	0.512	0.512	0.512	0.504	
a bond (Å)	2.5681	2.5586	2.5543	2.528	
b bond (Å)	2.5908	2.5812	2.5768	2.646	
c bond (Å)	3.7738	3.7617	3.7524	3.743	
d bond (Å)	3.7465	3.7293	3.7278	3.756	

lengths are nearly the same, the coordination number is 4 in practice, as in ZnTe I, and the band structure of ZnTe II turns out to be semiconducting, as expected. The calculated c and d bond lengths also agree with experiment well (Table II), which shows that our optimization procedure using the total energy, atomic forces, and stress tensors is working accurately beyond the nearest neighbors.

It is interesting to see how various atoms move when the first-order transition occurs from ZnTe I to ZnTe II. Although there is no unique way to describe the displacement of the virtually infinite number of atoms, we find the following simplified description helps visualize clearly the characteristic feature of the structural change. In Fig. 2(b), in comparison with the zinc-blende structure in (a), the bond of atoms 1-2 and that of atoms 2-3 rotate clockwise with respect to the [001] axis through atom 2 by 26° and 33°, respectively. By this rotation, atom 1 moves away from atom 13 and approaches atom 9. Identical rotation occurs for the bonds involving the atoms 8, 7, and 11 by translational symmetry. At critical pressure, the shortest bond length in the cinnabar structure is 2.568 Å compared with 2.541 Å for the zinc-blende structure, indicating that the strain accumulated by the applied pressure is relieved by the phase transition involving above-mentioned rotation. Adjustment of other bonds follows to minimize the overall enthalpy. For example, if we look at the ZnTe II structure along the [001] direction, the projected bond angles of atoms 4-7-5 and atoms 5-2-6 are 173.3° (i.e., buckled by 6.7° compared with the zinc-blende structure). We also note in Table II that atomic coordinate parameters (u for Zn and v for Te) obtained from our force and stress calculations remain constant under various pressures.

ZnTe III–orthorhombic ($Cmcm$) *phase*. The crystal structure of ZnTe III is orthorhombic with the space group $Cmcm$. The $Cmcm$ structure is a kind of distorted NaCl structures just as the cinnabar structure and the transition from the cinnabar to the $Cmcm$ is weakly first order. The bonding arrangement in ZnTe III may be regarded as (5+3) coordinated. In Fig. 2(c), around atom 1 (Zn), there are one a bond (1-10) of 2.6553 Å, two b bonds (1-2 and 1-9) of 2.7308 Å, and two c bonds (1-13 and 1-15) of 2.7154 Å. These five bonds have almost the same length. There are two d bonds of Zn-Zn contacts (1-11 and 1-12) of 3.0100 Å and one e bond of Zn-Te contact (1-17) of 3.0174 Å. With so many bonds of similar length, the band structure turns out to be metallic. In comparison with ZnTe II, atom 2 is pushed up in the [111] direction away from atom 6 and the bond of atoms 1-2 rotates clockwise by ~15° around the bond of atoms 5-2. The bond of atoms 2-3 also rotates clockwise by ~40° roughly around the bond of atoms 2-6. By these rotations, a shorter bond between atoms 1 and 13 is created. The same rotation occurs for the bonds involving the atoms 8, 7, and 11 by translational symmetry. At critical pressure, the shortest bond length in the $Cmcm$ structure is 2.655 Å, compared with 2.553 Å in the cinnabar structure, indicating that the strain is relieved by the phase transition into a more uniform and compact structure of higher coordination number. Table III compares the calculated structural parameters for the $Cmcm$ phase with experiment. According to our calculation, there is no more transition up to very high pressure (~100 GPa).

The wurtzite, NaCl, NiAs, β-tin, and CsCl structures are not to be realized in ZnTe. The NaCl structure exists in other tellurides (CdTe and HgTe) or zinc chalcogenides (ZnS and ZnSe). In CdTe (Ref. 2) and HgTe,[16] the cinnabar phase under pressure has been found to transform to the NaCl structure before going to the $Cmcm$ structure. The NaCl structure of ZnTe has a total energy only slightly above the $Cmcm$

TABLE III. The calculated lattice parameters (a,b,c), relative atomic coordinates y(Te) and y(Zn) and their difference for the $Cmcm$ phase of ZnTe at various pressures. Experimental results at 11.5 GPa and 15.7 GPa from Ref. 3 are given for comparison. Volumes are normalized to the calculated zero-pressure volume of the zinc-blende structure.

	Calculation				Experiment	
Volume	0.723	0.703	0.652	0.547		
Pres. (GPa)	10.23	13.29	24.02	62.58	11.5	15.7
a (Å)	5.3823	5.3408	5.2224	4.9493	5.436	5.379
b (Å)	6.0348	5.9881	5.8048	5.4020	6.050	5.971
c (Å)	5.0616	5.0042	4.8881	4.6558	5.058	5.010
y(Zn)	0.6350	0.6330	0.6310	0.6284		0.640
y(Te)	0.1950	0.1905	0.1830	0.1697		0.190
Δy	0.4400	0.4425	0.4480	0.4587		0.450

structure under low pressure, but the difference becomes larger as pressure increases (Fig. 1). We suspect that the greater imbalance in size between the cation and anion in ZnTe than in CdTe and HgTe favors the distorted structure over the higher-symmetry (cubic) NaCl structure. Recently, there was a report on the NaCl phase of ZnTe at combined high pressure and high temperatures.[17] It is not yet clear whether the free energy of the NaCl structure is actually lowered relative to that of the $Cmcm$ structure by heating. In the NiAs structure,[18] we find that interchanging the position of the anion (Te) and cation (Zn) further increases the total energy significantly (~0.5 eV/ZnTe). The β-tin phase that always exists in group IV semiconductors under pressure is too high in energy to be realized in ZnTe.

In summary, we present a microscopic study of the pressure-induced structural phase transition of ZnTe, employing the *ab initio* pseudopotential method within the LDA. Our calculation shows that the zinc-blende phase of ZnTe is the most stable one and it will transform to the cinnabar phase at 8.06 GPa and again to the $Cmcm$ phase at 10.24 GPa, in good agreement with experiment. The $Cmcm$ phase should be stable up to very high pressure (~100 GPa). Rotation of bonds to relieve the strain is identified at the critical pressure. The present study demonstrates that the *ab initio* pseudopotential total-energy (including the force and the stress tensor when necessary) calculation within the LDA can describe the pressure-induced phase transformation of crystals with the accuracy better than 1 mRy per atom in energy difference between different structures. Since we have carefully reduced the error originated from the pseudopotential method to within this amount, we conclude that the same number represents the upper bound of the error in the LDA; the LDA gives an extremely accurate description for the ground-state properties of non-strongly-correlated materials.

We are grateful to R. J. Nelmes, M. I. McMahon, N. G. Wright, and D. R. Allan for sending us their papers prior to publication. This work was supported by the BSRI Program of the Ministry of Education and the Korea Science and Engineering Foundation through the SRC Program.

---

[1] M. I. McMahon, R. J. Nelmes, N. G. Wright, and D. R. Allan, Phys. Rev. B **48**, 16 246 (1993).

[2] R. J. Nelmes, M. I. McMahon, N. G. Wright, and D. R. Allan, Phys. Rev. B **51**, 15 723 (1995).

[3] R. J. Nelmes, M. I. McMahon, N. G. Wright, and D. R. Allan, Phys. Rev. Lett. **73**, 1805 (1994).

[4] J. Ihm, A. Zunger, and M. L. Cohen, J. Phys. C **12**, 4409 (1979).

[5] O. H. Nielsen, and R. M. Martin, Phys. Rev. B **32**, 3792 (1985). We insert in Eq. (2) of this reference a missing term that takes into account the effect of the core charge.

[6] D. M. Bylander, L. Kleinman, and S. Lee, Phys. Rev. B **42**, 1394 (1990); **47**, 10 056 (1993).

[7] D. M. Ceperley and B. J. Alder, Phys. Rev. Lett. **45**, 566 (1980).

[8] J. P. Perdew and A. Zunger, Phys. Rev. B **23**, 5048 (1981).

[9] N. Troullier and J. L. Martins, Phys. Rev. B **43**, 1993 (1991).

[10] L. Kleinman and D. M. Bylander, Phys. Rev. Lett. **48**, 1425 (1982).

[11] X. Gonze, R. Stumpf, and M. Scheffler, Phys. Rev. B **44**, 4238 (1991).

[12] S. G. Louie, S. Froyen, and M. L. Cohen, Phys. Rev. B **26**, 2738 (1982).

[13] G. Ortiz and P. Ballone, Phys. Rev. B **43**, 6376 (1991).

[14] G. Lee, M. H. Lee, and J. Ihm, Phys. Rev. B **52**, 1459 (1995).

[15] N. G. Wright, M. I. McMahon, R. J. Nelmes, and A. San-Miguel, Phys. Rev. B **48**, 13 111 (1993).

[16] R. J. Nelmes, M. I. McMahon, N. G. Wright, and D. R. Allan, J. Phys. Chem. Solids **56**, 545 (1995).

[17] O. Shimomura (unpublished).

[18] S. Froyen and M. L. Cohen, Phys. Rev. B **28**, 3258 (1983).